Nonspecific Weak Actomyosin Interactions: Relocation of Charged Residues in Subdomain 1 of Actin Does Not Alter Actomyosin Function[†]

Wenise W. Wong, Timothy C. Doyle, and Emil Reisler*

Department of Chemistry and Biochemistry and Molecular Biology Institute, University of California, Los Angeles, California 90095

Received October 15, 1998

ABSTRACT: Yeast actin mutants with relocated charged residues within subdomain 1 were constructed so we could investigate the functional importance of individual clusters of acidic residues in mediating actomyosin weak-binding states in the cross-bridge cycle. Past studies have established a functional role for three distinct pairs of charged residues within this region of yeast actin (D2/E4, D24/D25, and E99/E100); the loss of any one of these pairs resulted in the same impairment in weak actomyosin interaction and in its function. However, the specificity of myosin interaction with these sites has not yet been addressed. To investigate this, we made and analyzed two new actin mutants, 4Ac/D24A/D25A and 4Ac/E99A/E100A. In these mutants, the acidic residues of the D24/D25 or E99/E100 sites were replaced with uncharged residues (alanines) and a pair of acidic residues was inserted at the N-terminus, maintaining the overall charge density of subdomain 1. Using the in vitro motility assays, we found that the sliding and force generation properties of these mutant actins were identical to those of wild-type actin. Similarly, actin-activated ATPase activities of the mutant and wild-type actins were also indistinguishable. Additionally, the binding of S1 to these mutant actins in the presence of ATP was similar to that of wild-type actin. These results show that relocation of charged residues in subdomain 1 of actin does not affect the weak actomyosin interactions and actomyosin function.

An understanding of the events leading to force generation in actomyosin requires a complete description of each of the actomyosin states in the cross-bridge cycle. These states fall into two main categories, the weakly and strongly bound actomyosin complexes. One of the important goals of muscle biochemistry is to clarify the transition between the weakly and strongly bound actomyosin states and to map the structural changes associated with this transition on myosin and actin and at their interface.

Structural models of acto-S1[1] (*1*−*3*) identified several elements of the two proteins which might bind to each other. These suggestions, which were based on both the results of prior biochemical studies and considerations of docking the atomic structure of S1 to the model of the F-actin structure, focused attention on the role of acidic clusters of residues 1−4, 24/25, and 99/100 in subdomain 1 of actin in myosin binding. Although it has been implicit to all acto-S1 models that weak binding of S1 to actin (in the presence of ATP) is dominated by electrostatic interactions (because of its strong dependence on ionic strength conditions), while the strong binding depends on hydrophobic acto-S1 interactions, these models could not predict the relative contributions of each of the three acidic residue sites on actin to the strong and weak acto-S1 binding. Immunochemical (*4*−*8*), biochemical (*9*−*11*), and mutational (*12*−*15*) studies shed light on this issue. They showed that D2/E4, D24/D25, and E99/E100 on yeast actin contribute to the weak acto-S1 binding while only the N-terminal acidic residues contribute also to the strong binding interactions (*14*, *15*).

An interesting result of the previous studies was that the loss of any one of these pairs of acidic residues on actin, either via substitution (DNEQ, D24A/D25A, and E99A/E100A) or deletion (ΔDSE, for deletion of D2, S3, and E4) had the same effect on the main parameters of actomyosin function. In all cases, the loss of two negative charges on actin decreased the binding constant for weak acto-S1 binding about 3-fold, decreased greatly the acto-S1 ATPase, and reduced the force generated against external load in the in vitro motility assays by about 30% (*14*, *15*). Experimentally, the most convenient consequence of the decreased weak myosin binding by these actin mutants was their inability to slide over HMM in the in vitro motility assays either in the absence of the viscosity-enhancing agent methylcellulose or under high ionic strength (100 mM) conditions (*14*, *15*). Under standard, low-salt conditions and in the presence of methylcellulose, the sliding speeds of these actin mutants were indistinguishable from that of wild-type actin.

The fact that the loss of two negative charges at any of the three sites (24/25, 99/100, and the N-terminus) in subdomain 1 of actin yields identical impairment of actomyosin function raises a question about the specificity of these weak electrostatic actomyosin interactions. These results suggest that such interactions are nonspecific and depend on the charge density of actin's subdomain 1 rather

[†] This work was supported by U.S. Public Health Service Grant AR22031 and NSF Grant MCB-9630997.

[1] Abbreviations: S1, myosin subfragment 1; HMM, heavy meromyosin; DNase I, deoxyribonuclease I; pPDM, *N*,*N*′-1,4-phenylenedimaleimide; F-actin, filamentous (polymerized) actin; 4Ac, yeast actin mutant with Asp and Glu inserted at the Ser3 position; DNEQ, yeast actin mutant with two residues substituted (D2N and E4Q); ΔDSE, yeast actin mutant with the three N-terminal residues deleted (Asp, Ser, and Glu).

10.1021/bi982467g CCC: $18.00
Published on Web 01/05/1999

FIGURE 1: Monomeric actin ribbon structure (*42*) with mutated amino acid residues depicted in space-filled form: 4Ac, light gray; 24/25, medium gray; and 99/100, dark gray.

than on the exact location of the acidic residues in that region. A simple test of this conclusion would involve the redistribution of negative charges among the three sites and the examination of functional properties of such charge relocated actin mutants. The results of previous studies (*15, 16*) paved the way for such experiments. These studies showed that addition of two negative charges at the N-terminus of yeast actin, to generate the 4Ac mutant with the N-terminus resembling that of the α-skeletal actin, does not change the weak and strong S1 binding to yeast actin or its sliding speed in the motility assays. Thus, the N-terminus of yeast actin provides a natural target site for relocation of acidic residues from the D24/D25 and E99/E100 sites on actin.

For this study, two new yeast actin mutants were generated, 4Ac/D24A/D25A and 4Ac/E99A/E100A (Figure 1). The loss of two negative charges at residues D24/D25 and E99/E100 in these actins is offset by addition of two acidic residues (Asp and Glu) at the N-terminus, with a zero overall net change in charge in subdomain 1. Using these charge relocation actin mutants, we show that the weak actomyosin interactions and their functional consequences are insensitive to the exact location of acidic residues in subdomain 1 and depend on the charge density of this region.

MATERIALS AND METHODS

Plasmid Construction and Yeast Transformation. The actin-coding regions for mutations D24A/D25A and E99A/E100A were amplified from plasmids pRB1554 and pRB1541, respectively [*act*1−133 and *act*1−120 (*17*), respectively] using Vent DNA polymerase (New England Biolabs, Beverly, MA). PCR using oligonucleotides 4Ac-term and C-term (GGCCGGATCCatgGAT*GAAGAT*GTTATGTTCTAGCGCTTGCACC and GGCCTCTAGAttaGAAACACTTGTGGTGAAC, respectively) introduced the 4Ac rabbit sequence to the 5′ end of the coding region (additional codons for the acidic residues are italicized), with *Bam*HI and *Xba*I cloning sites (underlined) flanking the start and stop codons (lowercase). The amplified product was digested with restriction enzymes *Bam*HI and *Xba*I (New England Biolabs) and run on a 1% agarose gel, and the DNA band was QIAEX II-purified (Qiagen, Valencia, CA). This fragment was ligated in the same sites of plasmid pTS422 (*18*). The presence of alanine scan mutations was confirmed by the presence of an additional *Fnu*4HI site, and the presence of the sequence encoding the 4Ac codons by the introduction of an additional *Hin*fI site. Amplified actin sequences were then sequenced (GeneMed, South San Francisco, CA) to confirm that no PCR-generated errors were introduced.

Plasmids were transformed (*19*) into the diploid yeast KWY201, which is heterozygous for a deletion of the ACT1 gene marked with an adjacent insertion of the LEU2 gene (*17, 20*), and selected by uracil independence. Transformed yeast strains were sporulated, and tetrad dissection was performed to separate the genomic-encoded wild-type actin-bearing haploids from those bearing the plasmid-borne mutant actin with the genomic actin deletion. The presence of the correct actin sequences in these strains was confirmed by PCR amplification of the actin gene, and *Fnu*4HI and *Hin*fI digestion as described above. The temperature phenotypes of strains bearing the mutant actin were determined by spotting aliquots of liquid culture on rich media plates, and incubation at 14, 17, 25, 30, 35, and 37 °C.

Preparation of Proteins. Yeast actin was isolated from each strain using DNase I affinity chromatography as described previously (*16*). To ensure the reproducibility of results, all yeast actins were used within 1 week of purification. Rabbit actin and myosin were prepared from rabbit skeletal muscle according to the methods of Spudich and Watt (*21*) and Godfrey and Harrington (*22*), respectively. Myosin S1 was prepared according to the methods of Weeds and Pope (*23*).

Cosedimentation Assays. Cosedimentation assays of the weak binding of S1 to 4.0 μM F-actin were carried out at 25 °C in 3.0 mM ATP, 4.0 mM $MgCl_2$, 10 mM NaCl, and 10 mM imidazole at pH 7.0 as previously described (*14*). ATP was added after the incubation of proteins for 10 min. The concentrations of S1 ranged between 5.0 and 40.0 μM. The protein samples were centrifuged at room temperature in a Beckman airfuge at 140 000 rpm for 14 min. Resuspended pellets and supernatants from each sample were examined by SDS−PAGE (*24*). Gels were stained with Coomassie Blue, and then scanned and quantified using Sigmagel (Jandel Scientific, Chicago, IL). The molar ratios of S1 bound to actin were obtained from these data and the appropriate calibration gels of protein stain.

Actin-Activated S1 ATPase Assays. Actin-activated ATPase activity was measured at 25 °C by using the malachite green assay (*25*). Due to assay sensitivity, free phosphate was removed from prepolymerized actin stock solutions as described previously (*12*). Actin samples at final concentrations of 5.0−40.0 μM were preincubated with 0.4 μM S1 for 20 min in the ATPase buffer (10 mM NaCl, 4.0 mM $MgCl_2$, and 10 mM imidazole at pH 7.0). The ATPase reaction was initiated by the addition of ATP to a final concentration of 3.0 mM. The reactions were stopped with an equal volume of 0.6 M perchloric acid, and then the mixtures were diluted appropriately while maintaining a final perchloric acid concentration of 0.3 M. The mixtures were centrifuged at 14 000 rpm for 10 min in a microcentrifuge to remove precipitated proteins. The amounts of released phosphate were determined and corrected for the activity of S1 alone as reported previously (*25*).

In Vitro Motility Assays. The motility assays were performed as previously described (*15*). The temperature was maintained at 25 °C for all assays. HMM was prepared as described by Kron et al. (*26*). To remove ATP-insensitive heads, HMM was centrifuged with 0.15 mg/mL rabbit F-actin in a solution containing 25 mM MOPS, 25 mM KCl, 1.0 mM $MgCl_2$, 10 mM DTT, and 4.0 mM ATP for 30 min at 75 000 rpm. The supernatant was applied to nitrocellulose-treated coverslips at an HMM concentration of 0.3 mg/mL, unless stated otherwise. Rhodamine phalloidin-labeled actin filaments were added to the coated coverslips at 20 nM, and after 30 s, the unbound filaments were washed away with the assay buffer (25 mM KCl, 1 mM EGTA, 4.0 mM $MgCl_2$, 10 mM DTT, and 10 mM imidazole at pH 7.4). The ionic strength of the high-salt buffer was adjusted to 100 mM with KCl. Movement was initiated with the assay buffer containing 1.0 mM ATP with an oxygen-scavenging system. Quantification of the sliding velocities was carried out with an Expertvision system (Motion Analysis, Santa Rosa, CA). The velocities of individual filaments with standard deviations of less than half of the average velocity were used for statistical analysis (*27*), and these filaments were considered to move smoothly in the assay system.

pPDM-HMM was prepared as described previously (*28*, *29*). The in vitro motility assays in the presence of pPDM-HMM load were performed as described above with the following modifications. HMM and pPDM-HMM at appropriate weight ratios were adsorbed to the assay surface for 2 min and washed off with 6 volumes of assay buffer to prevent contamination with unattached pPDM-HMM. Nonmoving filaments were identified by monitoring the centroid of each filament image with the Expertvision system and charting its position for 10 s.

RESULTS

Expression of Double-Site, Charge Relocation Yeast Mutant Actins. Yeast actin contains two acidic amino acids at the N-terminus, unlike the mammalian α-actin which contains four. The genomic sequence of the actin gene has an intron after the third codon immediately prior to the second acidic residue, and thus, only the first exon needs to be mutated from Met-Asp-Ser to the rabbit sequence Met-Asp-Glu-Asp. Amplification of the D24A/D25A and E99A/E100A mutant actins with primers that introduce this change allows the rapid generation of the double-site, charge relocation mutants 4Ac/D24A/D25A and 4Ac/E99A/E100A. These alleles produce viable actin proteins in yeast, and growth of the strains expressing these mutations shows a mild temperature sensitivity at elevated temperatures (results not shown).

Sliding of Actins in the in Vitro Motility Assays. Because of the striking effect of negative charge reduction at the N-terminus and residues 24/25 and 99/100 of yeast actin on its sliding in the absence of methylcellulose in the in vitro motility assays, we first examined the properties of the new mutants in these assays. Under standard buffer conditions of low ionic strength (50 mM) and in the presence of methylcellulose (0.7%), a viscosity-enhancing agent, the mutants moved in a manner identical to that of wild-type actin ($V_s = 3.0 \pm 0.3$ μm/s for wild-type, 4Ac/D24A/D25A, and 4Ac/E99A/E100A actins; Table 1). Under such conditions, actin mutants with the charged residues either removed or added to the subdomain 1 region of actin moved also at the speeds of wild-type actin (*16*).

Table 1: Sliding of Mutant Actin Filaments in the in Vitro Motility Assays[a]

yeast actin	speed (μm/s) 50 mM MC[b]	50 mM no MC	100 mM MC[b]
wild-type	3.0	2.7	1.6
4Ac/D24A/D25A	2.8	2.6	1.7
4Ac/E99A/E100A	3.0	2.6	1.5

[a] The motilities of actin filaments were measured as described in Materials and Methods. At least 100 filaments were analyzed for each sample. The standard deviation of the mean values was between 0.1 and 0.3 μm/s. [b] MC (0.7% methylcellulose) was included in the assay solution.

However, important changes in sliding of the charge-deficient mutants were observed when methylcellulose was omitted from the assay system or the ionic strength of the assay system was elevated. In the reported studies on the D24A/D25A, E99A/E100A, and DNEQ actins, the filament sliding ceased because the actin was rapidly diffusing away from the HMM surface (*15*). The sliding of wild-type actin was changed little, if any, by the lack of methylcellulose in the assay. Not surprisingly, as we found in this work, the sliding of 4Ac mutant actin was also unaffected by the presence or absence of methylcellulose. The 4Ac mutant actin filaments moved at speeds similar to that of wild-type actin ($V_s = 3.0 \pm 0.3$ μm/s) when no methylcellulose was present under low salt conditions, as well as under the higher-ionic strength condition (100 mM).

Most importantly, the sliding speeds of the 4Ac/D24A/D25A and 4Ac/E99A/E100A mutant filaments were identical to that of wild-type actin also in the absence of methylcellulose (Table 1). Thus, addition of the acidic residues to the N-terminus of actin in lieu of the acidic residues removed at either residues 24/25 or 99/100 "rescues" the motility of actin under conditions which do not favor weak actomyosin interactions (absence of methylcellulose or high salt). Clearly, relocation of charges on subdomain 1 of actin, unlike their loss, does not change the above tested motility properties of actin.

Weak Binding of Mutant Actins to S1. The weak binding of S1 to actin has been previously shown to be reduced by the loss of charged residues in subdomain 1 of actin (*14*, *15*). The affinities of the two actin mutants, 4Ac/D24A/D25A and 4Ac/E99A/E100A, and wild-type actin for S1 in the presence of ATP were determined in cosedimentation experiments. The resulting binding data are represented by a single binding curve corresponding to a K_d of 33.3 μM (Figure 2, dotted curve). The binding data for each of the actins were similar enough to fit to this single calculated curve; however, individual K_d values were calculated for each actin (32.9 ± 1.1 μM for the wild type, 38.3 ± 5.0 μM for 4Ac/D24A/D25A, and 32.8 ± 0.5 μM for 4Ac/E99A/E100A). Within the resolution and accuracy of these measurements, such small differences in the weak binding affinity of S1 for wild-type and mutant actins are insignificant.

Actin-Activated ATPase Activities. Kinetic parameters for actin-activated S1-ATPase of the wild-type actin and the two mutants 4Ac/D24A/D25A and 4Ac/E99A/E100A are summarized in Table 2. Again, a similarity between these two

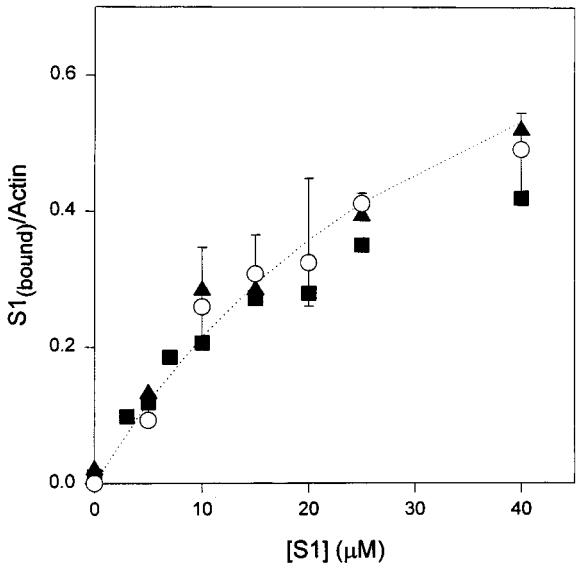

FIGURE 2: Binding of S1 to wild-type and mutant actins in the presence of MgATP. Mixtures of F-actin (4.0 μM) and S1 (between 5.0 and 40.0 μM) were pelleted in a Beckman airfuge at 140000*g* for 14 min in a solvent containing 10 mM NaCl, 10 mM imidazole, 4.0 mM $MgCl_2$, and 3.0 mM ATP at pH 7.0 and 22 °C. Supernatants and pelleted samples were run on SDS−PAGE and quantified by densitometry. The molar ratios of S1 bound to wild-type (○), 4Ac/D24A/D25A (■), and 4Ac/E99A/E100A (▲) F-actins are described by a single calculated curve corresponding to a K_d of 33.3 μM (dotted curve). Error bars represent the mean deviation from two independent experiments with each actin. For points which do not have error bars, the standard error was smaller than the size of the symbols.

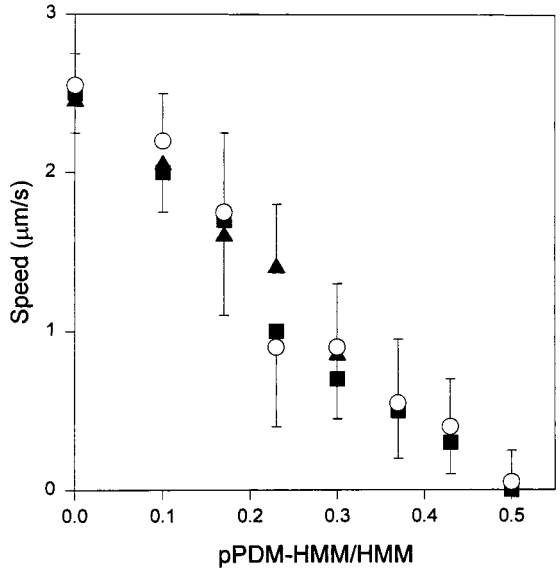

FIGURE 3: Sliding speeds of wild-type and mutant actins in the in vitro motility assays in the presence of external load. The sliding speeds of wild-type (○), 4Ac/E99A/E100A (■), and 4Ac/D24A/D25A (▲) yeast actins in the in vitro motility assays were measured as a function of the molar ratio of pPDM-HMM/HMM applied to the assay surface. Assays were carried out with a 0.3 mg/mL total HMM concentration applied to the coverslip, and the movement was initiated in the assay buffer [1 mM ATP, 25 mM MOPS (pH 7.4), 25 mM KCl, 1 mM EGTA, 4.0 mM $MgCl_2$, and 10 mM DTT]. At least 100 filaments were analyzed for each data point. For clarity of presentation, data points are shown with only half-values of the corresponding standard deviations.

Table 2: Kinetic Parameters of the Acto-S1 ATPase Reaction[a]

yeast actin	V_{max} (s^{-1})	K_{ATPase} (μM)
wild-type	2.2 ± 0.4	4.0 ± 0.4
4Ac/D24A/D25A	2.2 ± 0.5	4.9 ± 0.5
Ac/E99A/E100A	2.0 ± 0.5	4.9 ± 0.5

[a] Actin-activated ATPase of S1 was measured as described in Materials and Methods. V_{max} and K_{ATPase} values were determined by fitting the ATPase data to the Michaelis−Menten equation.

mutants was observed when compared to wild-type actin or against each other. The V_{max} of the mutants (2.1 ± 0.5 s^{-1}, Table 2) is nearly identical to the value determined for the wild-type actin (2.2 ± 0.4 s^{-1}, Table 2). Additionally, K_{ATPase} values for both mutants were nearly identical (K_{ATPase} = 4.9 ± 0.5 μM, Table 2) to that for wild-type actin (K_{ATPase} = 4.0 ± 0.4 μM, Table 2). This supports the conclusion derived from cosedimentation experiments that the weak binding of S1 to actin is similar for wild-type and 4Ac/D24A/D25A and 4Ac/E99A/E100A actins. In previous studies, V_{max} and K_m values could not be determined for the charge-deficient actin mutants because of the very low level of acto-S1 ATPases achieved with these actins.

Movement of Mutant Actins against Load. As reported previously (*15*), charge-deficient mutants of yeast actin generate about 30% less force, with HMM, than wild-type actin. The charge relocation mutants were used here to test whether the loss of force due to D24A/D25A or E99A/E100A substitutions could be reversed via additions of acidic residues to the N-terminus of actin. As in previous studies of this type (*15*, *30*−*34*), the ability of the mutant actins to generate force was tested in the in vitro motility assays in which pPDM-modified HMM was used as a source of weak external load on the motility surface. Because pPDM-HMM is unable to hydrolyze ATP and form the rigor actomyosin complex, the actin-bound pPDM-HMM heads create a load on the actin filament as it moves in the in vitro motility assay. When increasing proportions of pPDM-HMM are added to unmodified HMM in the assay system, an increasing load is generated, which the unmodified protein must overcome to move the filament. Thus, the relative amount of load that is needed to stop filament movement and relative forces developed by different actins can be determined in such assays.

The actin mutants 4Ac/D24A/D25A and 4Ac/E99A/E100A were tested independently in the in vitro motility assays in the presence of pPDM-HMM load, using wild-type actin as a control. Both actin mutants exhibited movement identical to that of wild-type actin at all pPDM-HMM:HMM ratios tested (Figure 3), i.e., generated the same force with HMM as wild-type actin. Clearly, the addition of two acidic residues at the N-terminus of actin corrected for the deficiencies in force generation due to alanine substitution of a pair of charged residues, either 24/25 or 99/100. This result agrees with and reinforces the conclusion derived from the other experiments presented here, including in vitro motility assays (no load), and weak acto-S1 binding and acto-S1 ATPase measurements about the lack of any functional distinction between wild-type actin and the charge relocation mutants.

DISCUSSION

The purpose of this study was to investigate the specificity of electrostatic contacts within the acto-S1 interface that are required for actomyosin interactions and actomyosin func-

tion. Previous experimental evidence that has led to questions about the specificity of weak acto-S1 interactions, which are known to be dominated by electrostatic forces, includes the observations on rotational mobility of S1 weakly bound to actin (*35*−*37*) and on different orientations of S1 on actin in the presence of ATP in electron micrographs of such complexes (*38*−*40*). The recent finding that charge deletions or substitutions of any one of the three pairs of acidic residues on yeast actin, D2/E4, D24/D25, and E99/E100, caused identical impairment of weak acto-S1 interactions and actomyosin function (*15*) added credence to the hypothesis that these interactions are nonspecific.

To provide a more stringent test of the specificity of weak myosin interactions with the three actin sites than that offered by charge-deficient actin mutants, two new actin mutants were generated in this work, 4Ac/D24A/D25A and 4Ac/E99A/E100A. The attractive features of these mutants are that they (i) do not alter the charge density of subdomain 1 on actin and (ii) "compensate" for aspartate to alanine (24/25) and glutamate to alanine (99/100) substitution by the replacement of S3 with two residues, aspartate and glutamate, to yield the 4Ac N-terminal sequence mimicking that of α-skeletal actin. The advantage of such charge relocation to actin's N-terminus is that prior work with the 4Ac yeast actin established that the additional charges at the N-terminus of actin do not impair its structure and do not change its weak binding to S1 and the in vitro motility under standard assay conditions (*16*, *41*).

The following question has been addressed using the two new actin mutants. Can the additional acidic residues at the N-terminus of actin (4Ac) compensate for the functional impairment of actin due to charge losses at sites 24/25 and 99/100? The assays we used in this study tested four interrelated manifestations of the decrease in the extent of weak acto-S1 interactions of D24/D25 and E99/E100 (as well as DNEQ and ΔDSE) yeast actins: (1) a 3-fold decrease in the extent of weak binding of S1 to actin, (2) a large decrease in the level of acto-S1 ATPase, (3) a loss of actin sliding in the in vitro motility assays under conditions requiring robust weak acto-S1 interactions (no methylcellulose or high ionic strength), and (4) decreases in force generation. In all of these, the 4Ac/D24A/D25A and 4Ac/E99A/E100A mutants were similar to wild-type actin and did not show any of the deficiencies of D24A/D25A and E99A/E100A actins.

The main result of this study is that relocation of charged residues in subdomain 1 of yeast actin to its N-terminus does not alter the functional properties of actomyosin. Weak actomyosin interactions are independent of charge distribution of acidic residues at sites 2/4, 24/25, and 99/100, and instead are determined by the charge density of the subdomain 1 region. Our results support the hypothesis that the electrostatic weak actomyosin interactions have only a limited stereospecificity (defined by a region rather than by individual groups of residues). The stereospecificity of actomyosin interactions, as suggested by structural models (*1*, *2*), must be achieved upon transition from the weakly to strongly bound actomyosin states.

REFERENCES

1. Rayment, I., Holden, H. M., Whittaker, M., Yohn, C. B., Lorenz, M., Holmes, K. C., and Milligan, R. A. (1993) *Science 261*, 58−65.
2. Schröder, R. R., Manstein, D. J., Jahn, W., Holden, H., Rayment, I., Holmes, K. C., and Spudich, J. A. (1993) *Nature 364*, 171−4.
3. Milligan, R. A. (1996) *Proc. Natl. Acad. Sci. U.S.A. 93*, 21−6.
4. Mejean, C., Boyer, M., Labbé, J. P., Marlier, L., Benyamin, Y., and Roustan, C. (1987) *Biochem. J. 244*, 571−7.
5. Miller, L., Kalnoski, M., Yunossi, Z., Bulinski, J. C., and Reisler, E. (1987) *Biochemistry 26*, 6064−70.
6. DasGupta, G., and Reisler, E. (1989) *J. Mol. Biol. 207*, 833−6.
7. DasGupta, G., and Reisler, E. (1991) *Biochemistry 30*, 9961−6.
8. DasGupta, G., and Reisler, E. (1992) *Biochemistry 31*, 1836−41.
9. Sutoh, K. (1982) *Biochemistry 21*, 4800−4.
10. Chaussepied, P., and Morales, M. F. (1988) *Proc. Natl. Acad. Sci. U.S.A. 85*, 7471−5.
11. Chaussepied, P. (1989) *Biochemistry 28*, 9123−8.
12. Sutoh, K., Ando, M., and Toyoshima, Y. Y. (1991) *Proc. Natl. Acad. Sci. U.S.A. 88*, 7711−4.
13. Johara, M., Toyoshima, Y. Y., Ishijima, A., Kojima, H., Yanagida, T., and Sutoh, K. (1993) *Proc. Natl. Acad. Sci. U.S.A. 90*, 2127−31.
14. Miller, C. J., and Reisler, E. (1995) *Biochemistry 34*, 2694−700.
15. Miller, C. J., Wong, W. W., Bobkova, E., Rubenstein, P. A., and Reisler, E. (1996) *Biochemistry 35*, 16557−65.
16. Cook, R. K., Root, D., Miller, C., Reisler, E., and Rubenstein, P. A. (1993) *J. Biol. Chem. 268*, 2410−5.
17. Wertman, K. F., Drubin, D. G., and Botstein, D. (1992) *Genetics 132*, 337−50.
18. Doyle, T., and Botstein, D. (1996) *Proc. Natl. Acad. Sci. U.S.A. 93*, 3886−91.
19. Ito, H., Fukuda, Y., Murata, K., and Kimura, A. (1983) *J. Bacteriol. 153*, 163−8.
20. Wertman, K. F., and Drubin, D. G. (1992) *Science 258*, 759−60.
21. Spudich, J. A., and Watt, S. (1971) *J. Biol. Chem. 246*, 4866−71.
22. Godfrey, J. E., and Harrington, W. F. (1970) *Biochemistry 9*, 886−93.
23. Weeds, A. G., and Pope, B. (1977) *J. Mol. Biol. 111*, 129−57.
24. Laemmli, U. K. (1970) *Nature 227*, 680−5.
25. Kodama, T., Fukui, K., and Kometani, K. (1986) *J. Biochem. 99*, 1465−72.
26. Kron, S. J., Uyeda, T. Q., Warrick, H. M., and Spudich, J. A. (1991) *J. Cell Sci., Suppl. 14*, 129−33.
27. Homsher, E., Wang, F., and Sellers, J. R. (1992) *Am. J. Physiol. 262*, C714−23.
28. Chalovich, J. M., Greene, L. E., and Eisenberg, E. (1983) *Proc. Natl. Acad. Sci. U.S.A. 80*, 4909−13.
29. Warshaw, D. M., Desrosiers, J. M., Work, S. S., and Trybus, K. M. (1990) *J. Cell Biol. 111*, 453−63.
30. Haeberle, J. R., and Hemric, M. E. (1994) *Can. J. Physiol. Pharmacol. 72*, 1400−9.
31. Haeberle, J. R. (1994) *J. Biol. Chem. 269*, 12424−31.
32. Haeberle, J. R., and Hemric, M. E. (1995) *Biophys. J. 68*, 306S−11S.
33. Homsher, E., Kim, B., Bobkova, A., and Tobacman, L. S. (1996) *Biophys. J. 70*, 1881−92.
34. Kim, E., Bobkova, E., Miller, C. J., Orlova, A., Hegyi, G., Egelman, E., Muhlrad, A., and Reisler, E. (1999) *Biochemistry* (in press).
35. Ostap, E. M., Barnett, V. A., and Thomas, D. D. (1995) *Biophys. J. 69*, 177−88.
36. Berger, C. L., and Thomas, D. D. (1994) *Biophys. J. 67*, 250−61.
37. Baker, J. E., Brust-Mascher, I., Ramachandran, S., LaConte, L. E., and Thomas, D. D. (1998) *Proc. Natl. Acad. Sci. U.S.A. 95*, 2944−9.

38. Walker, M., White, H., Belknap, B., and Trinick, J. (1994) *Biophys. J. 66*, 1563−72.
39. Fajer, P. G., Fajer, E. A., Schoenberg, M., and Thomas, D. D. (1991) *Biophys. J. 60*, 642−9.
40. Pollard, T. D., Bhandari, D., Maupin, P., Wachsstock, D., Weeds, A. G., and Zot, H. G. (1993) *Biophys. J. 64*, 454−71.
41. Cook, R. K., Blake, W. T., and Rubenstein, P. A. (1992) *J. Biol. Chem. 267*, 9430−6.
42. Kabsch, W., Mannherz, H. G., Suck, D., Pai, E. F., and Holmes, K. C. (1990) *Nature 347*, 37−44.

BI982467G